# Optical Absorption of a D2+ Artificial Molecule Confined in a Spherical Quantum Dot

**Emre Bahadir Al**
Sivas Cumhuriyet University
**Huseyin Sari** ( sari@cumhuriyet.edu.tr )
Sivas Cumhuriyet University
**Serpil Sakiroglu**
Dokuz Eylul University: Dokuz Eylul Universitesi
**İsmail Sokmen**
Dokuz Eylul University: Dokuz Eylul Universitesi

**Research Article**

**Keywords:** Quantum dot, Impurity, Artificial molecule, Optical transitions

**Posted Date:** January 12th, 2022

**DOI:** https://doi.org/10.21203/rs.3.rs-1004538/v1

# Optical absorption of a $D_2^+$ artificial molecule confined in a spherical quantum dot

E. B. Al[1], H. Sari[2a], S. Sakiroglu[3] and I. Sökmen[3]
[1] *Sivas Cumhuriyet University, Faculty of Science, Physics Department, 58140 Sivas, Turkey*
[2] *Sivas Cumhuriyet University, Faculty of Education, Department of Mathematics and Natural Science Education, 58140 Sivas, Turkey and*
[3] *Dokuz Eylul University, Faculty of Science, Physics Department, 35390 Izmir, Turkey*
(Dated: October 21, 2021)

In this work, we have performed a theoretically study on the energy spectrum, binding energy and intersubband optical absorption of a $D_2^+$ complex confined in a spherical quantum dot with finite confinement potential by using diagonalization method within the effective mass approximation. We analyzed the effect of the quantum dot size and internuclear distance on the binding energy, equilibrium distance and optical response of the singly ionized double donor complex. Theoretical analysis of the $D_2^+$ system indicated that the internuclear distance significantly affects the energy difference between the two lowest-lying electron states and amplitude of the optical absorption. In general, we conclude that the internuclear distance and quantum dot size dependence of the low-lying energy spectrum of the $D_2^+$ complex in a quantum dot favors the describing of an appropriate two-level system needed for quantum computation.

Keywords: Quantum dot; Impurity; Artificial molecule; Optical transitions

## I. INTRODUCTION

In recent years, investigation of electronic and optical properties of low-dimensional semiconductor systems in which carriers' movement freedom is restricted has gained importance. In this context, many studies have been carried out to determine the basic properties of quantum dots (QDs), also called artificial atoms [1, 2], in which the particles are confined in three directions. This strong confinement in QDs gives them unique properties and allows them to be considered as ideal systems for next generation optoelectronic devices such as lasers, photodetectors, amplifiers and solar cells.

Up to date, the studies have shown that the electronic structure and optical response of impurity trapped in these zero-dimensional structures exhibits interesting properties [3–8]. For instance, in the study on the current progress in III-V QD based optoelectronic devices by Wu et al [4], it was stated that doping in the active region plays a critical role in the performance of QD infrared photodetectors. The energy spectrum and corresponding eigenfunctions of the hydrogenic donor confined in a square QD is investigated by Pavlović in a four level ladder configuration [5]. The obtained results are used to analyze the effects of the confinement and the laser field on the electromagnetically induced transparency and it is emphasized that the absorption peak width is a non-monotonic function of the confinement of the hydrogenic impurity. On the other hand, Bera et al studied the modulation of electro-optical effect and nonlinear optical sensitivity of the impurity doped QD in the presence of noise with Gaussian distribution [6]. In their study, it was noted that the effect of dopant location could hardly be observed in the absence of noise and in the presence of additive noise. Nonlinear optical responses of doped QDs have been performed by Ghosh et al in presence of Gaussian white noise with fixed and spatially varying effective mass by modelling the impurity potential via a Gaussian function [8]. In their work, it is emphasized that the noise effect on the nonlinear optical response becomes more pronounced for the spatially varying effective mass case.

Advances in the single-doping technique [9–11] and charge detection [12, 13] have led to increased interest in another molecular system consisting of two confined donor impurities in a semiconductor host where one of the two excess electrons is ionized. In this context, the studies on the electronic structure and related properties of $H_2^+$-like impurities confined in QDs have been carried out [14, 15]. Particularly, Kang et al have introduced a variational method to calculate the energy spectra of the $H_2^+$-like impurities confined by spherical QDs as a function of the nuclear distance for different geometric sizes of the structure [14]. In this study, a quantitative analysis of the ground and some low-lying energy states is presented. In another study, they proposed a scheme for realizing a charge qubit consisting of ground and first excited states of a confined double-donor system by spherical $GaAs - Ga_{1-x}Al_xAs$ QDs [15]. They have found that under suitable physical conditions, $H_2^+$-like impurities confined in QDs can be considered as a quasi-two-level system, and the localized impurity states of this system can be used as charge qubits. This two-level

[a] Corresponding author (H. Sari): sari@cumhuriyet.edu.tr

system encodes logical information on the spin or charge degrees of freedom of a single electron and allows us to tune its molecular properties accordingly [16–22]. The effect of spatial and dielectric confinements on the electron charge distribution, spontaneous emission rates, and transition energies of a singly ionized double donor system ($D_2^+$) in a QD are calculated by Movilla et al using the effective-mass approximation [23]. They reported that the confinement of the $D_2^+$ system in a QD provides additional possibilities to tune its properties such as the charge distribution of the lowest-lying states, the corresponding energy splittings, and the radiative lifetimes. The energies and eigenfunctions of a singly ionized $D_2^+$ complex in vertically coupled QDs in the presence of a magnetic field were calculated by Manjarres-Garcia et al using a variational separation of variables for different structure morphologies [24]. Recently, Xu and colleagues performed a pump-probe experiment to investigate electron localization in the dissociation of the $H_2^+$ molecule and breaking a chemical bond in real time [25]. The experimental results obtained in their studies were also supported by a theoretical simulation based on the numerical solution of the time-independent equation.

Motivated by the importance of coupled donor impurities in nanotechnology applications, in this study we focus on the energy spectra, binding energy and intersubband optical absorption of a $D_2^+$ artificial molecule confined in a spherical quantum dot with finite confinement potential. We investigate the effect of both the nuclear distance and the QD size on the energy spectra, the binding energy, the molecular dissociation energy and optical absorption coefficients (OACs).

The present study is organized as follows: In Sec. II, we introduce the physical model of the singly ionized $D_2^+$ complex confined in the QD and outline the details of the numerical method used to solve the resulting eigenvalue equation. The obtained results are presented and discussed in Sec. III, and our conclusions are given in Sec. IV.

## II. THEORETICAL FRAMEWORK

### A. $D_2^+$ complex

In the framework of the effective mass and parabolic band approximation, the Hamiltonian of the $D_2^+$ complex in the spherical QD can be written as

$$H = -\frac{\hbar^2}{2m^*}\nabla^2 + V_{QD}(r) + V_{DD} + V_C\,, \tag{1}$$

where, $m^*$ is the effective mass of the electron in the QD material, $r$ is the distance from the electron to center of QD. For simplicity, we assume that one of the two positive donors is located at the center of the $GaAs/Ga_{1-x}Al_xAs$ QD and the other donor is located at the $D$-position on the $z$-axis. $V_{QD}(r)$ is the spherically symmetric confinement potential and it is defined as [26]

$$V_{QD}(r) = \begin{cases} 0, & r < R \\ V_0, & r \geq R \end{cases}, \tag{2}$$

where, $V_0 = Q_c\Delta E_g$ is the barrier height, $R$ is the QD radius, $Q_c = 0.6$ is conduction band offset parameter and $\Delta E_g = 1247x\,(meV)$ [27] is the difference between the band gaps of $Ga_{1-x}Al_xAs$ and $GaAs$ QD materials and depends on the aluminum alloy concentration ($x$) in $Ga_{1-x}Al_xAs$.

$V_{DD}$ is the donor-donor repulsive Coulomb potential and it is written as

$$V_{DD} = \frac{e^2}{\varepsilon D}, \tag{3}$$

where, $e$ is the absolute value of the electronic charge and $\varepsilon$ is the effective dielectric permeability of the QD.

$V_C$ is the attractive Coulomb interaction potential between electron and donors and it is given by

$$V_C = -Z\frac{e^2}{\varepsilon}\left(\frac{1}{|\vec{r}-\vec{D}|} + \frac{1}{r}\right), \tag{4}$$

where, $Z = 0$ ($Z = 1$) indicates the case without (with) electron-donor interactions.

The term $\frac{1}{|\vec{r}-\vec{D}|}$ is given in terms of spherical harmonics by

$$\frac{1}{|\vec{r}-\vec{D}|} = \sum_{\mu}\frac{4\pi}{2\mu+1}f_\mu(r)\sum_{\nu=-\mu}^{\mu}Y^*_{\mu,\nu}(\theta,\phi)Y^*_{\mu,\nu}(\theta_D,\phi_D), \tag{5}$$

where, $\theta$ and $\phi$ ($\theta_D$ and $\phi_D$) are the polar angles of the electron (impurity atom), and $f_\mu(r)$ is

$$f_\mu(r) = \begin{cases} \frac{1}{D}(\frac{r}{D})^\mu, & r \leq D \\ \frac{1}{r}(\frac{D}{r})^\mu, & r \geq D \end{cases}. \tag{6}$$

As the distance between the donors becomes very large ($D \to \infty$), we can see that the coupling between the two impurities is weak and they behave like two separate isolated hydrogenic impurities. But when $D$ is very small ($D \to 0$), the coupling between the two impurities will be very large and the total potential energy is very similar to the potential energy of an electron around a single dopant with a double doping charge, i.e. the $He^+$ atom-like impurity state.

If the lengths and energies are taken in terms of the effective Bohr radius ($a_B = \frac{\hbar^2\varepsilon}{m^* e^2}$) and the effective Rydberg constant ($R_y^* = \frac{\hbar^2}{2m^* a_B^2}$), respectively, the total Hamiltonian is obtained in dimensionless form

$$H = -\nabla^2 + V_{QD}(r) + \frac{2}{D} - 2Z\left(\sum_\mu \frac{4\pi}{2\mu+1} f_\mu(r) \sum_{\nu=-\mu}^{\mu} Y^*_{\mu,\nu}(\theta,\phi) Y^*_{\mu,\nu}(\theta_D,\phi_D) + \frac{1}{r}\right), \tag{7}$$

where, $\nabla^2$ is the Laplace operator.

To determine the energy eigenvalues and eigenfunctions of the system, we must solve the Schrödinger equation

$$H\psi_{nlm}(r,\theta,\phi) = E_{nlm}\psi_{nlm}(r,\theta,\phi)\,, \tag{8}$$

where, $n$ is the principal, $l$ is the angular momentum and $m$ ($-l \leq m \leq l$) is the magnetic momentum quantum numbers. This equation is not analytically solvable, so we use the diagonalization method to calculate the eigenfunctions and corresponding eigenvalues. Therefore, we choose a linear combination of trial envelope wavefunctions representing the electron in the infinite spherical QD [28]

$$\psi_{nlm}(r,\theta,\phi) = \sum_j c_{n_j,l_j}\psi^{(0)}_{n_j l_j m}(r,\theta,\phi), \tag{9}$$

where $c_{n_j,l_j}$ are the expansion coefficients, $\psi^{(0)}_{n_j l_j m}(r,\theta,\phi)$ is the total wavefunction describing the motion of the electron without impurity atoms and it is written in terms of radial wavefunction and spherical harmonics due to the spherical symmetry of the system as

$$\psi^{(0)}_{nlm}(r,\theta,\phi) = \varphi^{(0)}_{nl}(r)Y_{lm}(\theta,\phi), \tag{10}$$

where the radial wave function-$\varphi^{(0)}_{nl}(r)$ is given as

$$\varphi^{(0)}_{nl}(r) = \begin{cases} N j_l(k_{nl}r), & r < R_i \\ 0, & r \geq R_i \end{cases}, \tag{11}$$

where $R_i$ ($R_i >> R$) is the radius of the infinite spherical QD, $N$ is the normalization constant and $k_{nl}$ is the $n$th root of $l$th order spherical Bessel functions.

Since the ionization process is $D_2^+ \to D^+ D^+ + e^-$, the binding energy of $D_2^+$ is given by

$$E^b_{nlm} = E_{nlm}(Z=0) - E_{nlm}(Z=1), \tag{12}$$

where, $E_{nlm}(Z=0)$ and $E_{nlm}(Z=1)$ are the energies without and with electron-donor interactions, respectively.

### B. Linear and nonlinear optical absorption

The optical transition that occurs by the absorption of a photon between the initial and final states is known as the photo-absorption method. As electromagnetic radiation passes through the QD, OACs provide information about the reduction in radiation intensity. To calculate the various optical properties, we need to consider the interaction between the polarized electromagnetic wave with angular frequency $\omega$ and the QD ensemble (Fermi's Golden Rule) [29].

OAC is considered an important parameter for optical transitions. To investigate OACs, the optical transition energy between the two states studied is calculated. Using the density matrix formalism and the perturbative procedure, the analytical expressions of the linear, third-order nonlinear and total OACs for a two-level quantum system interacting with a monochromatic optical field are given respectively by

$$\alpha^{(1)}(\omega) = \sqrt{\frac{\mu}{\varepsilon_r}} \frac{\sigma_s \Gamma_{ij}}{(E_{ij} - \hbar\omega)^2 + (\hbar\Gamma_{ij})^2} \hbar\omega |M_{ij}|^2, \tag{13}$$

$$\alpha^{(3)}(\omega, I) = -\sqrt{\frac{\mu}{\varepsilon_r}} \left(\frac{2I}{n_r \varepsilon_0 c}\right) \frac{\sigma_s \Gamma_{ij} \hbar\omega |M_{ij}|^4}{[(E_{ij} - \hbar\omega)^2 + (\hbar\Gamma_{ij})^2]^2} \left[1 - \frac{|M_{jj} - M_{ii}|^2 [3E_{ij}^2 - 4E_{ij}\hbar\omega + \hbar^2(\omega^2 - \Gamma_{ij}^2)]}{4|M_{ij}|^2 (E_{ij}^2 + (\hbar\Gamma_{ij})^2)}\right] \tag{14}$$

and

$$\alpha(\omega, I) = \alpha^{(1)}(\omega) + \alpha^{(3)}(\omega, I), \tag{15}$$

where, $\mu = \frac{1}{\varepsilon_0 c^2}$ is the magnetic permeability of the system ($\varepsilon_0$ and $c$ are the permittivity and light speed of the vacuum), $\varepsilon_r = n_r^2 \varepsilon_0$ is the real part of the dielectric permittivity of the material, $n_r$ is the static component of the refractive index in QD, $\sigma_s$ is the electron density of the QD, non-diagonal matrix element $\Gamma_{ij}$ is the phenomenological relaxation ratio operator caused by electron-phonon, electron-electron and other collision processes and it is the inverse of relaxation time-$\tau_{ij}$, $E_{ij} = E_j - E_i$ is the energy difference between the levels in two level systems, $\hbar\omega$ is the energy of the incident photon, $I = 2\varepsilon_0 n_r c|\tilde{E}|^2$ is the intensity of the incident resonant light ($|\tilde{E}|$ is the amplitude of the incident light), and $M_{ij}$ are the dipole moment matrix elements between the initial and final states in QD and they can be calculated from

$$M_{ij} = \langle \psi_i | er\cos\theta | \psi_j \rangle, \tag{16}$$

where $\psi_i$ and $\psi_j$ are wave functions representing the electron at the initial and final levels.

The $M_{jj} - M_{ii}$ term causes a small effect on the nonlinear OAC around the resonance when any of the donor atoms is outside the center of the QD. Since this effect is very small, the contribution from the second term of the parenthesis in Eq. 14 can be neglected. However, this term must be taken into account when considering its essential roles on incident photon energies outside the resonance region. For linear OAC the resonance condition is $\hbar\omega = \sqrt{E_{ij}^2 + (\hbar\Gamma_{ij})^2}$ whereas for nonlinear OAC it is $\hbar\omega = \frac{1}{3}\left(E_{ij} + \sqrt{4E_{ij}^2 + 3(\hbar\Gamma_{ij})^2}\right)$ [26]. In this case, the maximum values of linear and nonlinear OACs are given respectively by

$$\alpha^{(1)}(\omega) = \sqrt{\frac{\mu}{\varepsilon_r}} \frac{e^2 \sigma_s \Gamma_{ij}}{(E_{ij} - \hbar\omega)^2 + (\hbar\Gamma_{ij})^2} \Omega_1 \tag{17}$$

and

$$\alpha^{(3)}(\omega, I) = -\sqrt{\frac{\mu}{\varepsilon_r}} \left(\frac{2I}{n_r \varepsilon_0 c}\right) \frac{e^4 \sigma_s \Gamma_{ij}}{[(E_{ij} - \hbar\omega)^2 + (\hbar\Gamma_{ij})^2]^2} \Omega_2 \tag{18}$$

where, $\Omega_1 = e^{-2}\sqrt{E_{ij}^2 + (\hbar\Gamma_{ij})^2}|M_{ij}|^2$ and $\Omega_2 = \frac{e^{-4}}{3}\left(E_{ij} + \sqrt{4E_{ij}^2 + 3(\hbar\Gamma_{ij})^2}\right)|M_{ij}|^4$ are the main parameters that determine the amplitudes of the linear and nonlinear OACs.

According to the minimum energy rule, not every possible transition in the absorption spectrum can be observed. In addition to the conservation of energy, the conservation of angular momentum and some symmetry rules must also be provided. Due to the azimuth symmetry of the system and the property of spherical harmonics, dipole transitions in spherical QDs are only allowed between states satisfying the $\Delta l = \pm 1$ and $\Delta m = 0, \pm 1$ selection rules. The selection rules determine the final state of the electron after absorption. All allowed transitions are included in the dipole matrix elements, i.e. optical transitions are allowed when the dipole matrix element is not zero. In this study, we only considered $m = 0$ states.

## III. RESULTS AND DISCUSSION

At this stage, we report the obtained energy states, binding energy and intersubband OACs of a $D_2^+$ artificial molecule confined in a spherical QD with finite confinement potential for different values of the QD size and internuclear distance values. The used physical parametres are: $\varepsilon = 13.18$, $a_B = 10.4\,nm$, $R_y^* = 5.23\,meV$, $V_0 = 224.46\,meV$,

$m^* = 0.067m_0$ (where $m_0 = 9.10956 \times 10^{-31}\,kg$ is the mass of free electron), $T_{ij} = 0.14\,ps$, $\mu = 4\pi \times 10^{-7}\,H/m$, $n_r = 3.2$, $\sigma_s = 1 \times 10^{23}\,m^{-3}$ and $I = 400\,MW/m^2$.

In Fig. 1, we display variation of the total energy of the $D_2^+$ complex (total energy of the electron plus the donor-donor Coulomb repulsion) corresponding to the $1s$ and $1p$ states as a function of the internuclear distance for four different values of QD size ($R = 10,\ 30,\ 50$ and $100\ nm$). From this figure, it is possible to conclude that increasing the QD size leads to greater dissociation energy and greater internuclear equilibrium distance for both the $1s$ and $1p$ states. Such that for $R = 10\ nm$ the internuclear equilibrium distance and dissociation energy corresponding to the $1s$ state are respectively $5\ nm$ and $9.32\ meV$ while for $R = 100\ nm$ these values get to be $11\ nm$ and $-8.22\ meV$. This means that as the QD width decreases, the kinetic energy of the electron increases and becomes more energetic, therefore the $D_2^+$ complex gets to be disassociated. It is apparent that similar behavior is in question for the $1p$ state. Nevertheless, for each value of $R$ considered, the $1p$ state is lying above the $1s$ state. The effect of QD size on the electronic structure of the $D_2^+$ complex is seen in more detail in Table I. Comparing the variation of the $1s$ and $1p$ states, it appears that the QD dimension-$R$ is more influential on the $1p$ state. Also, notice that for sufficiently large QD width values, the effect of the geometric confinement negligibly weakens while that of the nuclear would buildup. Therefore, in the case of sufficiently large internuclear distance and QD width values (for sufficiently large values of both $R$ and $D$ parameters), the $D_2^+$ complex turns into two isolated donor atoms with the sole electron ending up on one of the two nuclei.

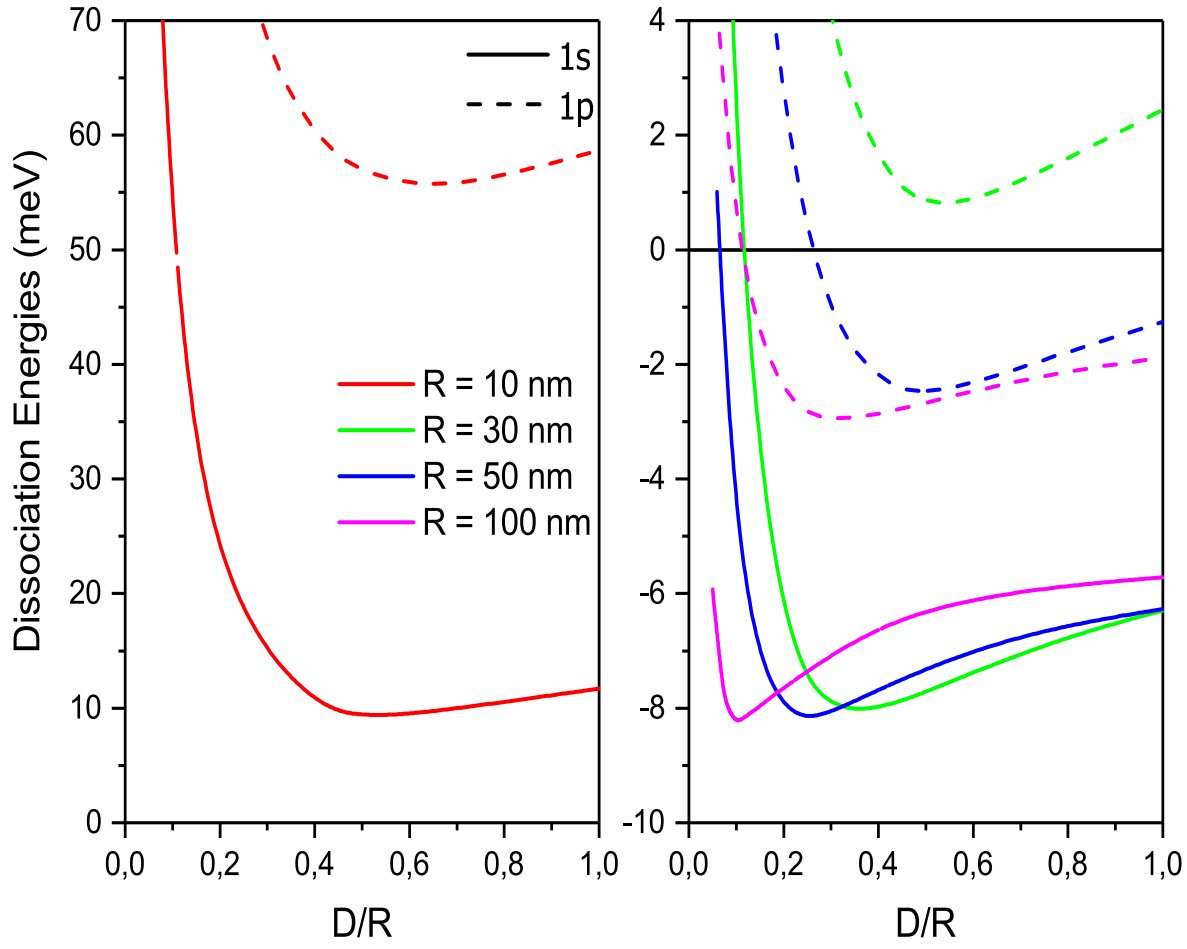


FIG. 1. (color online) Variation of the dissociation energies of the $D_2^+$ complex corresponding to the $1s$ and $1p$ states as a function of internuclear distance for four different QD size values ($R = 10,\ 30,\ 50$ and $100\ nm$).

The variation of binding energies corresponding to the $1s$ and $1p$ states of the $D_2^+$ complex as a function of the QD radius-$R$ is presented in Fig. 2 for several different values of the internuclear distance. As can be clearly seen in the

TABLE I. Effect of QD size on the electronic structure of the $D_2^+$ complex.

| Quantum Size | Equilibrium Distance | $1s$ | Equilibrium Distance | $1p$ |
|---|---|---|---|---|
| $R$ $(nm)$ | $D$ $(nm)$ | Dissociation Energy $(meV)$ | $D$ $(nm)$ | Dissociation Energy $(meV)$ |
| 10 | 5 | 9.31627 | 6 | 55.7187 |
| 30 | 9 | -8.0469 | 15 | 0.78249 |
| 50 | 10 | -8.29435 | 25 | -2.49879 |
| 100 | 11 | -8.22969 | 30 | -3.00058 |

figure, for all $D$ values considered, the binding energy corresponding to the $1s$ state reaches its maximum value at about $R = 8\ nm$. The reason for this is that when QD is at this width value, the spatial confinement takes its strongest value. Depending to the symmetry of the wave function representing the $1p$ state, the binding energy corresponding to the $1p$ state becomes maximum at larger $R$ values compared to the $1s$ state. On the other hand, another point that should be emphasized is that in cases where the internuclear distance parameter-$D$ is very small, the $D_2^+$ system will exhibit similar behavior to the hydrogen-like $He^+$ atom defined in three-dimensional space for sufficiently large and small values of the parameter-$R$. This behavior is clearly seen when examining the curve for $D = 1\ nm$ in Fig. 2. Indeed, the binding energy corresponding to the $1s$ state for $D = 1\ nm$ converges to approximately the same value $\approx 20\ meV$ at sufficiently small and large $R$ values. This value is closer to the value $23.32\ meV$ corresponding to the 3D binding energy of the hydrogen-like $He^+$ atom ($E_b(\mathrm{He}^+) = (\frac{Z}{n})^2 R_y^* = 4R_y^*$) [30]. The difference between both results can be understood by considering the fact that there is a small distance between two impurity atoms. Also, for $D = 1\ nm$ and $R = 100\ nm$, the binding energy of the $D_2^+$ corresponding to the first excited energy level $1p$ is about $6.35\ meV$, and this value is very close to the binding energy value corresponding to the first excited state ($E_b(\mathrm{He}^+) = 5.83\ meV$, for $n = 2$) of the hydrogen-like $He^+$ atom. Also note that when the distance between impurity atoms is large enough, the $D_2^+$ complex is reduced to a single isolated hydrogenic impurity atom case. For example, in the case of $D = 100\ nm$, and $R = 100\ nm$, the binding energy value corresponding to the $1s$ state is $E_b = 1.3R_y^*$. These assessments show that the method we used in the present study provides a realistic description of the energy spectrum of the $D_2^+$ complex confined in a spherical QD.

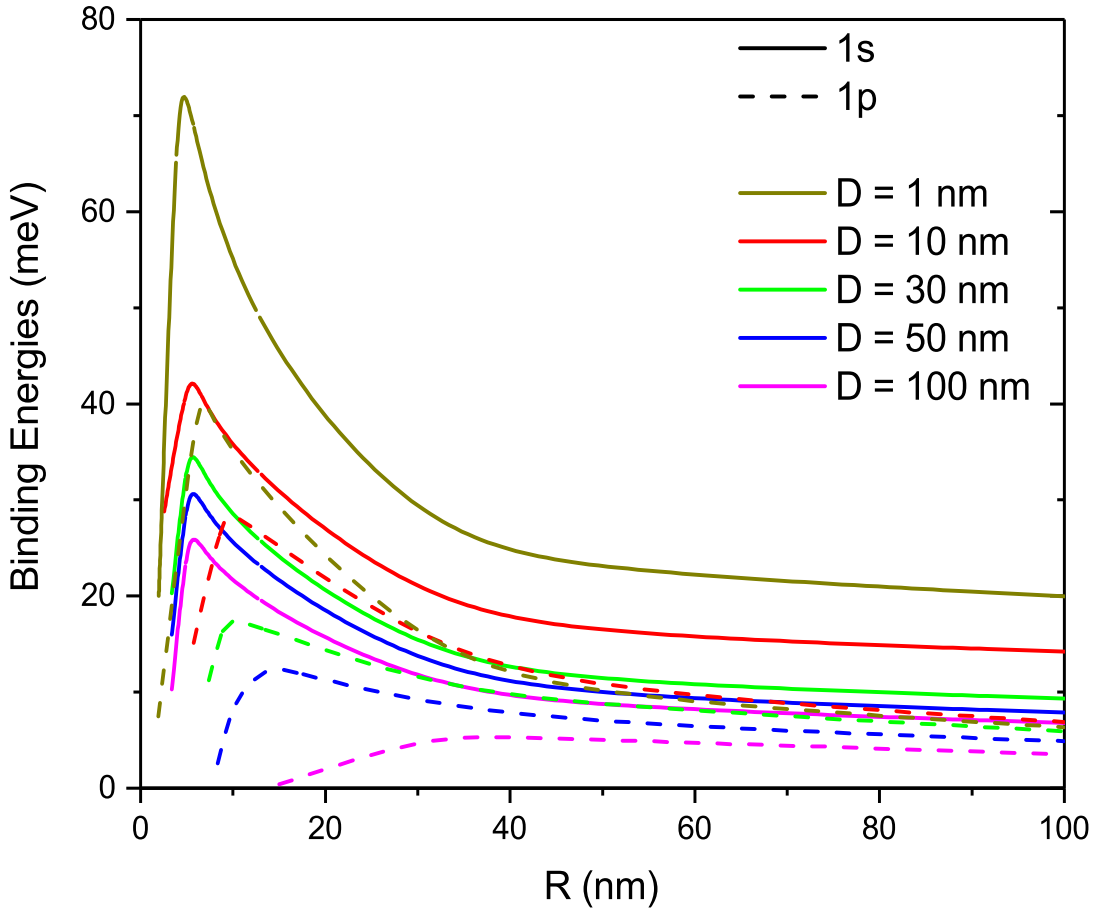


FIG. 2. (color online) Variation of binding energies corresponding to the $1s$ and $1p$ states of the $D_2^+$ complex as a function of QD radius-$R$ for several different values of the internuclear distance.

In Fig. 3, we show the evolution of the linear, third-order nonlinear and total intersubband ($1s \rightarrow 1p$) OACs related to the $D_2^+$ complex confined in a spherical QD for different values of the confinement size-$R$ and internuclear distance-$D$. In general, as the value of nuclear distance increases, it is observed that for narrow QDs the peak position of OACs shifts towards larger photon energies, whereas for wider QDs it is redshifted. We can clarify this feature as follows: Since the $1p$ energy state in narrow QDs is rather large compared to the $1s$ state, this state is less affected by the change of the Coulombic potential term in the base of the geometric confinement than the $1s$ state. Therefore, as can be seen in Fig. 1, the $1s$ energy state changes drastically with increasing internuclear distance-$D$, while the $1p$ state changes less, resulting in a significant increase in the energy difference $E_{ij}$. However, in large QDs where the quantum confinement is weak, both energy states change almost at the same rate and accordingly, the energy difference-$E_{ij}$ decreases as the internuclear distance increases. To illustrate this behavior in more detail, the variation of the related energy difference-$E_{ij}$ is presented in Fig. 4 (a) as a function of internuclear distance. It is apparent that as mentioned above the internuclear dependence of the energy difference-$E_{ij}$ is significant in the strong confinement regime compared to that of weak geometric confinement case. By analyzing Fig. 3 in detail, especially at large $D$ values, it is determined that while the amplitude of linear OACs decreases with $R$, that of third-order nonlinear OACs increases, and as a result, the amplitude of total OACs decreases with the QD size. On the other hand, for the values of $R = 10\ nm$ and $30\ nm$ the OACs increases with the parameter-$D$ while in the case of large QD size ($R = 100\ nm$) the opposite behavior is observed. In order to visualize the variation in the amplitudes of the OACs depending on the QD size and internuclear distance, the variations of the $\Omega_1$ and $\Omega_2$ factors are presented in Fig. 4 (b) and (c) as a function of the parameter-$D$. As can be seen in this figure, while the $\Omega_1$ factor which affects the peak amplitude of the linear OAC decreases with increasing values of $D$ for $R = 100\ nm$, it increases significantly for the other values

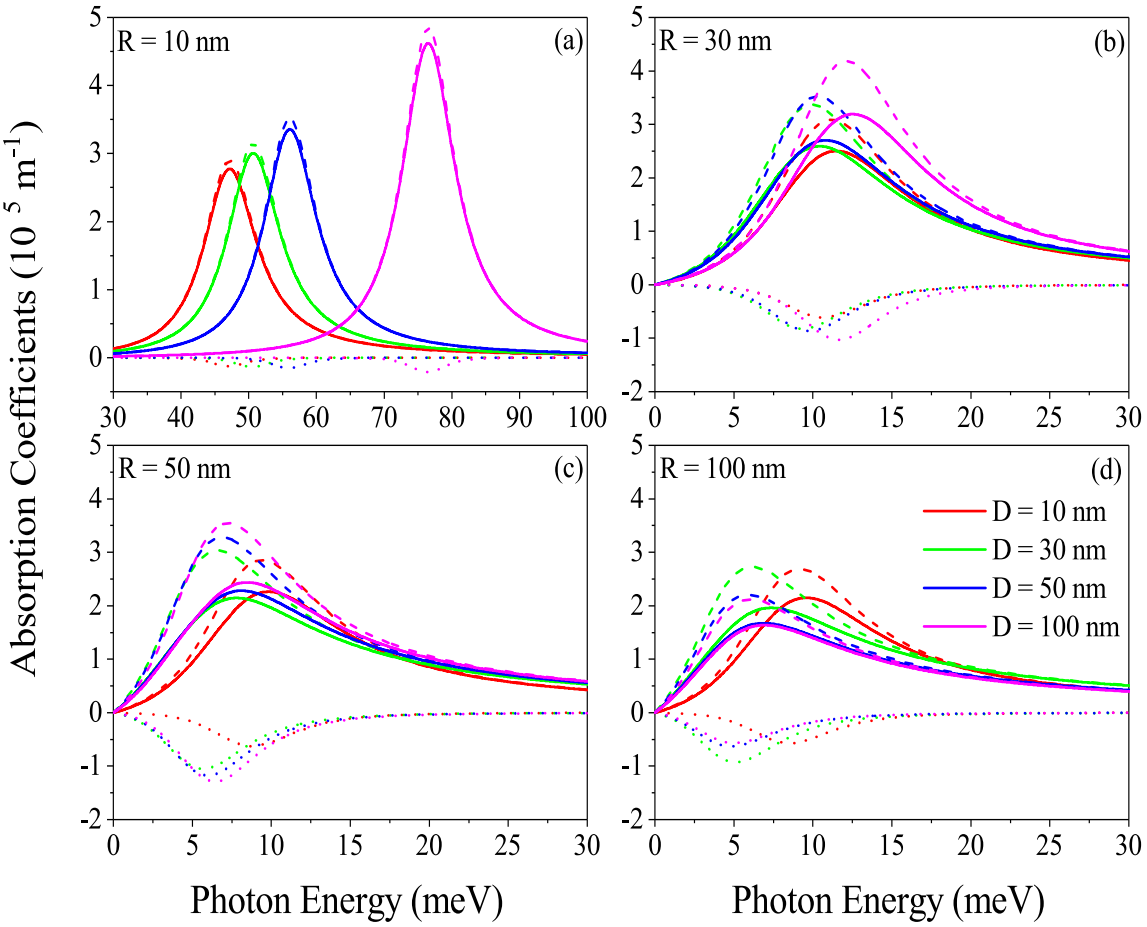


FIG. 3. (color online) Variation of linear, third-order nonlinear and total intersubband ($1s \rightarrow 1p$) OACs with respect to incident photon energy related to the $D_2^+$ complex confined in a spherical QD for different values of confinement size-$R$ and internuclear distance-$D$.

of $R$ considered. Similarly, the $\Omega_2$ factor which affects the peak amplitude of the nonlinear OAC increases with the parameter-$D$ for $R = 10\ nm$, $30\ nm$, and $50\ nm$. But for $R = 100\ nm$, it first increases rapidly with the $D$ parameter and then it decreases radically in the range of $D > 20\ nm$. Based on these results, it can be concluded that the QD size and internuclear distance have significant influence on the optoelectronic properties of the $D_2^+$ complex confined in a spherical QD.

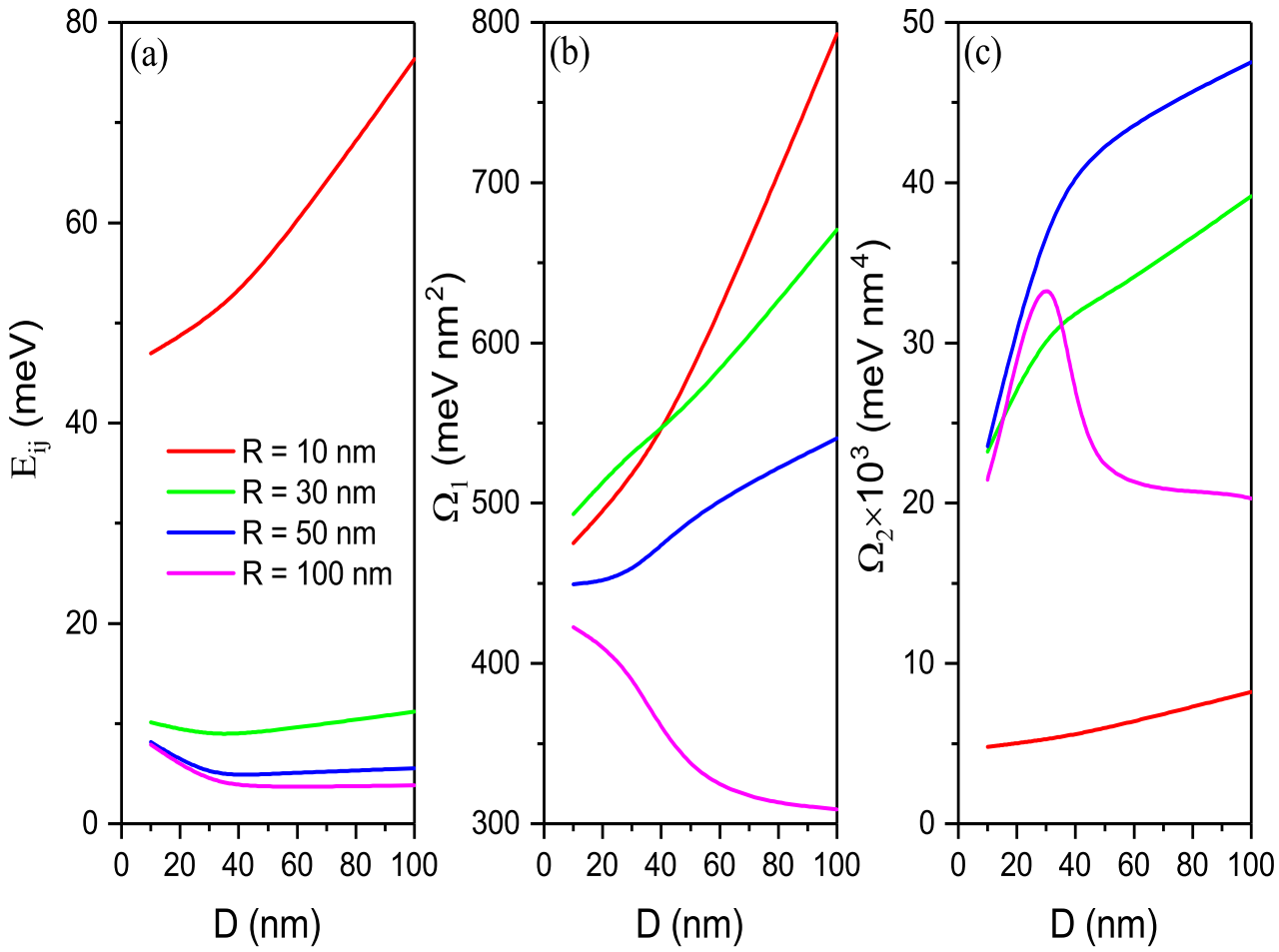


FIG. 4. (color online) Variation of $\Omega_1$ and $\Omega_2$ factors as well as energy difference depending on QD size and internuclear distance.

## IV. CONCLUSIONS

We have performed a theoretically study on the energy spectrum and optical intersubband transitions of the $D_2^+$ complex confined in a spherical QD. We analyzed the effect of the QD size and internuclear distance on the binding energy, equilibrium distance and optical response of the singly ionized double donor complex. Theoretical analysis of the $D_2^+$ system indicated that the internuclear distance significantly affects the energy difference between the two lowest-lying electron states and amplitude of the optical absorption, especially in the case of the strong quantum confinement regime. The internuclear distance and QD size dependence of the low-lying energy spectrum of the $D_2^+$ complex in a QD favors the describing of an appropriate two-level system needed for quantum computation purposes. Also, in the case of weak geometric confinement, the results obtained for very small internuclear separation are comparable with the results obtained for the hydrogen-like $He^+$ atom defined in three-dimensional space.

[1] S. Bednarek, B. Szafran and J. Adamowski, *Many-electron artificial atoms*, Phys. Rev. B **59**, 13036–13042 (1999).

[2] S. -J. Cheng, W. Sheng and P. Hawrylak, *Theory of excitonic artificial atoms: InGaAs/GaAs quantum dots in strong magnetic fields*, Phys. Rev. B **68**, 235330 (2003).

[3] D. Bimberg, M. Grundmann and N. Ledentsov, *Quantum Dot Heterostructures*, 1st edition, Chichester : John Wiley, 344 (1999).

[4] J. Wu, S. Chen, A. Seeds and H. Liu, *Quantum dot optoelectronic devices: lasers, photodetectors and solar cells*, J. Phys. D: Appl. Phys. **48**, 363001 (2015).

[5] V. Pavlović, *Electromagnetically induced transparency in a spherical quantum dot with hydrogenic impurity in a four level ladder configuration*, Optik **127**, 6351–6357 (2016).

[6] A. Bera, J. Ganguly, S. Saha and M. Ghosh, *Interplay between noise and position-dependent dielectric screening function in modulating nonlinear optical properties of impurity doped quantum dots*, Optik **127**, 6771–6778 (2016).

[7] R. M. Abolfath, *Para-ortho transition of artificial $H_2$ molecule in lateral quantum dots doped with magnetic impurities*, Phys. Rev. B **80**, 165332 (2009).

[8] A. P. Ghosh, A. Mandal, S. Sarkar and M. Ghosh, *Influence of position-dependent effective mass on the nonlinear optical properties of impurity doped quantum dots in presence of Gaussian white noise*, Opt. Commun. **367**, 325-334 (2016).

[9] J. L. O'Brien, S. R. Schofield, M. Y. Simmons, R. G. Clark, A. S. Dzurak, N. J. Curson, B. E. Kane, N. S. McAlpine, M. E. Hawley and G. W. Brown, *Towards the fabrication of phosphorus qubits for a silicon quantum computer*, Phys. Rev. B **64**, 161401(R) (2001).

[10] S. R. Schofield, N. J. Curson, M. Y. Simmons, F. J. Ruess, T. Hallam, L. Oberbeck and R. G. Clark, *Atomically Precise Placement of Single Dopants in Si*, Phys. Rev. Lett. **91**, 136104 (2003).

[11] T. Shinada, S. Okamoto, T. Kobayashi and I. Ohdomari, *Enhancing semiconductor device performance using ordered dopant arrays*, Nature **437**, 1128–1131 (2005).

[12] R. J. Schoelkopf, P. Wahlgren, A. A. Hozhevnikov, P. Delsing and D. E. Prober, *The Radio-Frequency Single-Electron Transistor (RF-SET): A Fast and Ultrasensitive Electrometer*, Science **280**, 1238-1242 (1998).

[13] A. Aassime, G. Johansson, G. Wendin, R. J. Schoelkopf and P. Delsing, *Radio-Frequency Single-Electron Transistor as Readout Device for Qubits: Charge Sensitivity and Backaction*, Phys. Rev. Lett. **86**, 3376 (2001).

[14] S. Kang, Y. -M. Liu and T. -Y. Shi, *The characteristics for $H_2^+$-like impurities confined by spherical quantum dots*, Eur. Phys. J. B **63**, 37-42 (2008).

[15] S. Kang, Y. -M. Liu and T. -Y. Shi, *$H_2^+$-Like Impurities Confined by Spherical Quantum Dots: a Candidate for Charge Qubits*, Commun. Theor. Phys. **50**, 767-770 (2008).

[16] M. J. Calderón, B. Koiller and S. Das Sarma, *External field control of donor electron exchange at the $Si/SiO_2$ interface*, Phys. Rev. B **75**, 125311 (2007).

[17] M. J. Calderón, B. Koiller, X. Hu and S. Das Sarma, *Quantum Control of Donor Electrons at the $Si/SiO_2$ Interface*, Phys. Rev. Lett. **96**, 096802 (2006).

[18] L. C. L. Hollenberg, A. S. Dzurak, C. Wellard, A. R. Hamilton, D. J. Reilly, G. J. Milburn and R. G. Clark, *Charge-based quantum computing using single donors in semiconductors*, Phys. Rev. Lett. **69**, 113301 (2004).

[19] A. V. Tsukanov, *Single-qubit operations in the double-donor structure driven by optical and voltage pulses*, Phys. Rev. B **76**, 035328 (2007).

[20] L. A. Openov, *Resonant pulse operations on the buried donor charge qubits in semiconductors*, Phys. Rev. B **70**, 233313 (2004).

[21] B. Koiller, X. Hu and S. Das Sarma, *Electric-field driven donor-based charge qubits in semiconductors*, Phys. Rev. B **73**, 045319 (2006).

[22] S. D. Barrett and G. J. Milburn, *Electric-field driven donor-based charge qubits in semiconductors*, Phys. Rev. B **68**, 155307 (2003).

[23] J. L. Movilla, A. Ballester and J. Planelles, *Coupled donors in quantum dots: Quantum size and dielectric mismatch effects*, Phys. Rev. B **79**, 195319 (2009).

[24] R. Manjarres-García, G. E. Escorcia-Salas, I. D. Mikhailov and J. Sierra-Ortega, *Singly ionized double-donor complex in vertically coupled quantum dots*, Nanoscale Research Letters **7**, 489 (2012).

[25] H. Xu, Z. Li, F. He, X. Wang, A. Atia-Tul-Noor, D. Kielpinski, R. T. Sang and I. V. Litvinyuk, *Observing electron localization in a dissociating H2+ molecule in real time*, Nat. Commun. **8**, 15849 (2017).

[26] E. B. Al, E. Kasapoglu, H. Sari and I. Sökmen, *Optical properties of spherical quantum dot in the presence of donor impurity under the magnetic field*, Physica B **613**, 412874 (2021).

[27] S. Adachi, *GaAs, AlAs, and $Al_xGa_{1-x}As$: Material parameters for use in research and device applications*, J. Appl. Phys. **58**, R1 (1985).

[28] E. B. Al, E. Kasapoglu, H. Sari and I. Sökmen, *Zeeman splitting, Zeeman transitions and optical absorption of an electron confined in spherical quantum dots under the magnetic field*, Phil. Mag. **101**, 117-128 (2021).

[29] G. Rezaei, M. R. K. Vahdani and B. Vaseghi, *Nonlinear optical properties of a hydrogenic impurity in an ellipsoidal finite potential quantum dot*, Curr. Appl. Phys. **11**, 176-181 (2011).

[30] Y. A. Suaza, M. R. Fulla, D. Laroze, H. M. Baghramyan and J. H. Marin, *Intense laser field effect on $D_2^+$ molecular complex localized in semiconductor quantum wells*, Chem. Phys. Lett. **730**, 384-390 (2019).